



Cite this: *Environ. Sci.: Processes Impacts*, 2023, 25, 2001

## Canadian high arctic ice core records of organophosphate flame retardants and plasticizers†

Amila O. De Silva, \*<sup>a</sup> Cora J. Young, \*<sup>b</sup> Christine Spencer,<sup>a</sup> Derek C. G. Muir, <sup>a</sup> Martin Sharp, <sup>c</sup> Igor Lehnerr <sup>d</sup> and Alison Criscitiello <sup>c</sup>

Organophosphate esters (OPEs) have been used as flame retardants, plasticizers, and anti-foaming agents over the past several decades. Of particular interest is the long range transport potential of OPEs given their ubiquitous detection in Arctic marine air. Here we report 19 OPE congeners in ice cores drilled on remote icefields and ice caps in the Canadian high Arctic. A multi-decadal temporal profile was constructed in the sectioned ice cores representing a time scale spanning the 1970s to 2014–16. In the Devon Ice Cap record, the annual total OPE ( $\sum$ OPEs) depositional flux for all of 2014 was  $81 \mu\text{g m}^{-2}$ , with the profile dominated by triphenylphosphate (TPP,  $9.4 \mu\text{g m}^{-2}$ ) and tris(2-chloroisopropyl) phosphate (TCPP,  $42 \mu\text{g m}^{-2}$ ). Here, many OPEs displayed an exponentially increasing depositional flux including TCPP which had a doubling time of  $4.1 \pm 0.44$  years. At the more northern site on Mt. Oxford icefield, the OPE fluxes were lower. Here, the annual  $\sum$ OPEs flux in 2016 was  $5.3 \mu\text{g m}^{-2}$ , dominated by TCPP ( $1.5 \mu\text{g m}^{-2}$ ) but also tris(2-butoxyethyl) phosphate ( $1.5 \mu\text{g m}^{-2}$  TBOEP). The temporal trend for halogenated OPEs in the Mt. Oxford icefield is bell-shaped, peaking in the mid-2000s. The observation of OPEs in remote Arctic ice cores demonstrates the cryosphere as a repository for these substances, and supports the potential for long-range transport of OPEs, likely associated with aerosol transport.

Received 19th May 2023  
Accepted 12th October 2023

DOI: 10.1039/d3em00215b

rsc.li/epsi

### Environmental significance

Ice cores from icefields from high altitude, uninhabited areas in the Canadian high Arctic were used to determine temporal trends of twenty-five organophosphorus flame retardants and plasticizers (OPEs). The depositional flux to the Devon Ice Cap for many OPEs is exponentially increasing over nearly four decades. Some were associated with anthropogenic particles. In the more northern site, annual flux was lower. The cryosphere is a repository for OPEs and may have implications for climate-induced release.

## 1 Introduction

Organophosphate esters (OPEs) are used as flame retardants, plasticizers, and anti-foaming agents with production occurring for the past several decades.<sup>1</sup> Applications of OPEs vary and include furniture, textiles, electronics, building materials, vehicle, and petroleum industries with OPEs being typically

incorporated as additives. Evaluating the environmental fate and transport of OPEs has emerged as a priority.<sup>2</sup> The presence of OPEs in indoor and outdoor air, sediment, water,<sup>3,4</sup> wastewater,<sup>5</sup> and biota<sup>6</sup> including human urine<sup>7</sup> and breast milk<sup>8</sup> is confirmed.

OPEs have been detected in the urban atmosphere and precipitation<sup>4</sup> but also in polar and other remote areas in fresh snow,<sup>9–11</sup> air, and aerosols.<sup>12,13</sup> Ocean–atmosphere exchange studies demonstrate marine (aerosol and dissolved) transport of OPEs is also a relevant long range transport pathway with 5 to  $20 \text{ ng L}^{-1} \sum_{11} \text{OPE}$  in water and 200 to  $1000 \text{ pg m}^{-3}$  in the gas phase in paired air samples from the Bering Strait between 65 and 80 °N latitude.<sup>14</sup> Recently, OPEs were observed in Lake Hazen and its glacier-fed tributaries on northern Ellesmere Island (Nunavut, Canada), downstream of the Mt. Oxford icefield coring location of this study.<sup>15</sup> These observations are suggestive of long range transport potential of OPEs. Their relatively low molecular weight and intermediate polarity may contribute to their atmospheric presence as well as a propensity

<sup>a</sup>Aquatic Contaminants Research Division, Environment Canada, 867 Lakeshore Road, Burlington, ON L7S 1A1, Canada. E-mail: amila.desilva@ec.gc.ca; Christine.spencer0501@gmail.com; derek.muir@ec.gc.ca

<sup>b</sup>Department of Chemistry, York University, Toronto, ON, M3J 1P3, Canada. E-mail: youngcj@yorku.ca

<sup>c</sup>Department of Earth and Atmospheric Sciences, University of Alberta, Edmonton, AB, T6G 2R3, Canada. E-mail: crisciti@ualberta.ca; msharp@ualberta.ca

<sup>d</sup>Department of Geography, Geomatics and Environment, University of Toronto Mississauga, Mississauga, Ontario L5L 1C6, Canada. E-mail: igor.lehnerr@utoronto.ca

† Electronic supplementary information (ESI) available. See DOI: <https://doi.org/10.1039/d3em00215b>



to deposition. Earlier studies proposed that OPEs were not candidates for long range transport based on empirical and modeled physical properties coupled with low environmental persistence.<sup>16,17</sup> Emerging studies suggest that these traditional approaches to evaluating long range transport potential based on gas phase transport are not entirely applicable to OPEs and that aerosol-based transport may be a key mechanism.<sup>17,18</sup>

While OPEs are widely reported in the abiotic Arctic environment, surveys of OPEs in Arctic marine biota indicate very little accumulation in tissues. For example, monitoring of OPEs in the blubber or adipose tissues from whales, seals, walrus, polar bears and glaucous gulls indicated very low detection frequencies and only sporadic detection of low concentrations of a few OPEs with TCPP having the highest detection frequency of 30–55% and only in two species of whale.<sup>19</sup> The limited profile of OPEs in Arctic biota is attributed to their low bio-persistence as OPEs undergo both phase I and phase II metabolism.<sup>19,20</sup> High dose acute exposure to OPEs induces toxic effects but less is known about environmentally-relevant doses.<sup>18,20</sup>

The purpose of this research is to evaluate the temporal trends in OPEs deposition to the high Arctic by examining their profile in ice cores. In addition, we sought to evaluate the long range atmospheric transport potential of OPEs as the ice cores were sampled from uninhabited inland regions in the high Arctic. To this end, we report OPEs in ice cores sampled from Devon Ice Cap and Mount Oxford icefield in Arctic Canada (Fig. 1).

Devon Ice Cap is on Devon Island, an uninhabited island in the Arctic archipelago spanning 55 000 km<sup>2</sup>. It is at extreme northern latitude (75°N) and the highest point of the ice cap

where sampling occurred is at an elevation of 2200 m. The Mt. Oxford icefield is further north at 82°N on Ellesmere Island in the Grant Lands mountain range, and has a peak elevation of 2210 m. We have previously reported temporal deposition of perfluoroalkyl substances (PFAS), brominated flame retardants and pesticides in ice from Devon Ice Cap<sup>21–25</sup> and more recently, ultra short chain perfluoroalkyl carboxylates from both Devon Ice Cap and Mt. Oxford icefield.<sup>26</sup> In addition to the extensive and continuous timescales they capture, ice cores have additional benefits. Active air sampling requires an uninterrupted power supply and therefore limits the remoteness of the feasible sampling locations. In addition, setting up active or passive samplers for multi-year data requires more long-term labour and introduces greater uncertainty between inter-year comparisons.

Contaminants on the Devon Ice Cap and Mt Oxford icefield are expected to be the result of atmospheric deposition due to (1) the low proximity to point sources, (2) distance from the ocean, and (3) high altitude. Here, we examine the temporal deposition of OPEs using the depth profile of OPEs in a dated ice core from the summits of Devon Ice Cap (1979–2015) and Mt. Oxford icefield (1975–2017).

## 2 Methods

### 2.1 Study sites and sampling

The Devon Ice Cap has an area of approximately 14 000 km<sup>2</sup>, located on the eastern side of Devon Island (Fig. 1). The accumulation rate at the summit of the ice cap is approximately 30 cm water equivalent/year and mean annual temperature is –23 °C.<sup>27</sup> At its deepest point, the ice is 880 m thick. The cores

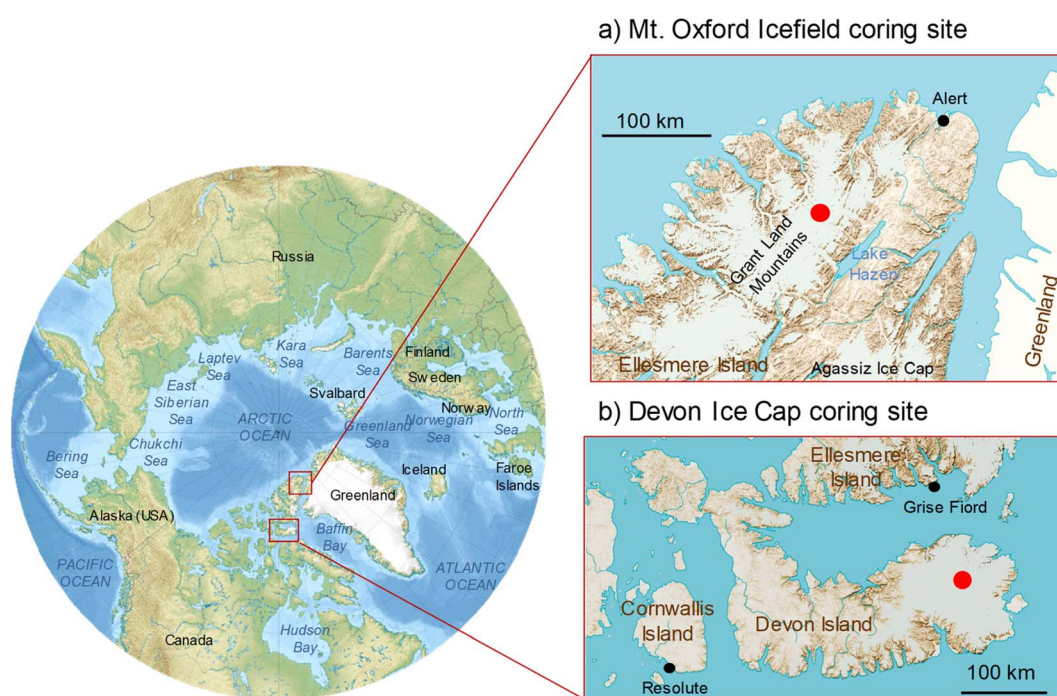


Fig. 1 Study area in Arctic Canada. Insets indicate coring sites (red circles) on Ellesmere Island in the Mount Oxford icefield and the Devon Ice Cap on Devon Island. Map from royalty-free and non-exclusive license at atlas.gc.ca, Natural Resources Canada.



were drilled on May 17, 2015 at the summit of the ice cap (75.3434°N, 82.1290°W) at 2200 m above sea level. Sampling was conducted as previously described using a 9 cm diameter commercially available stainless steel ice core drill (Kovacs Mark II).<sup>26</sup> The same drill was used for ice coring in both sites and does not contain any plastic parts that are in contact with the ice core. The entire rind of the core was removed and discarded. Thus, any firn or ice that was touching the inner circumference of the barrel is removed to minimize any contamination.

The Mt. Oxford icefield is located in Quttinirpaaq National Park, northern Ellesmere Island (Fig. 1). The icefield is part of a larger 12 000 km<sup>2</sup> glaciated area, the Grant Land Mountains.<sup>28</sup> The coring site was located at the summit, 82.1790°N, 72.9555°W, and was chosen due to its higher latitude, altitude, and inland location. Mt. Oxford icefield has an annual accumulation rate of approximately 10 cm water equivalent according to the age–depth scale found in this study, consistent with other reports.<sup>29,30</sup> Ellesmere Island is mostly uninhabited with the exception of the settlement of Grise Fiord, population 129, at the southern end of the island, as well as two high Arctic weather stations. Approximately 250 km southwest of the coring site is the Eureka weather station (79.9892°N, 85.9339°W). At approximately 164 km northeast of the coring site at 82.5017°N, 62.3481°W, is the high Arctic weather station and Canadian Forces station, Alert, located at sea level. The annual mean temperature at the coring site is likely even lower than that of Eureka which is at 10 m above sea level and has an annual mean temperature of −17 °C ([https://climate.weather.gc.ca/historical\\_data/search\\_historic\\_data\\_e.html](https://climate.weather.gc.ca/historical_data/search_historic_data_e.html)). Cores were drilled on May 26, 2017 using a 7.7 cm diameter mechanical drill.

At both sites, additional cores were drilled within 5 m for dating purposes and other contaminant analysis.<sup>23</sup> The bottom ages of the cores were determined in the field using a down-hole gamma spectrometer. This technique is based on the horizon markers of <sup>137</sup>Cs and <sup>239</sup>Pu associated with the global atmospheric fall out of nuclear weapons testing with maximum fallout corresponding to 1963. The development and validation of this technique have been previously described.<sup>31,32</sup> The length of the core represented approximately 36 years of deposition (1979 to 2015) in the Devon Ice Cap and 42 years of deposition (1975 to 2017) in the Mt. Oxford icefield. Note: the year of sampling only represents 5.5 months of accumulation and not a full year. Core sections were transferred to polyethylene tubing, secured in insulated ice core boxes, and shipped frozen to the laboratory facility in Burlington, Ontario.

Back trajectory air mass density analysis was calculated using the NOAA Hybrid Single-Particle Lagrangian Integrated Trajectory (HySPLIT) model. Ten-days back trajectories were calculated over an entire year using National Centers for Environmental Protection and Atmospheric Research global atmospheric reanalysis with a focus on low-elevation air masses (0–500 m above terrain) as they are representative of evaporation moisture sources as described previously.<sup>33,34</sup> Other time spans have also been used for back trajectories such as 3 and 5 days in other research but 10 days has been used for many years

including early work by Kahl *et al.*<sup>35</sup> and more recently.<sup>36</sup> Total trajectory endpoints were summed for each equal area pixel and then divided by the zonal distance between the ice coring site and each pixel to remove concentric patterning. The transport density results were scaled to 0–1 for comparison. This approach was developed specifically for interpretation of polar ice core paleoclimate records and has been found to derive more reliable airflow pathways that discriminate between local circulation patterns and regional scale flow features.<sup>33</sup> The approach is considered more reliable than single back trajectory analysis regardless of 3, 5, or 10 days back trajectories, which were shown to result in position errors up to 20%.<sup>33</sup> The approach was applied to two years, of no particular significance, 2001 and 2013, for each location.

## 2.2 Glaciochemistry

Studies have shown that despite surface summer melt, seasonal glaciochemical cycles are preserved in the ice, and therefore, core chemistry can be used to interpret interannual variability.<sup>37</sup> Dating of the ice cores has been described previously and a brief overview is provided herein.<sup>23</sup> The cores designated for dating from Devon Ice Cap and Mt. Oxford icefield were 19 m and 14 m in length, respectively. Cores were analyzed using a continuous flow analysis system in 1 cm intervals with ion chromatography to determine the major ion concentrations (Na<sup>+</sup>, Cl<sup>−</sup>, Mg<sup>2+</sup>, Ca<sup>2+</sup>, NH<sub>4</sub><sup>+</sup>, K<sup>+</sup>, NO<sub>3</sub><sup>−</sup>, and SO<sub>4</sub><sup>2−</sup>), high resolution inductively coupled plasma mass spectrometry for simultaneous analysis of 30 elements and fluorescence spectroscopy for detection of H<sub>2</sub>O<sub>2</sub> at the Desert Research Institute in Reno, Nevada using previously reported methods.<sup>23,34,38</sup> Oxygen (<sup>18</sup>O) isotope analysis was by cavity ring-down spectroscopy (Picarro, Santa Clara, CA, USA) with precision <0.1% for δ<sup>18</sup>O. The δ<sup>18</sup>O depth measurements were used to establish an age–depth relationship and accumulation rates by matching the δ<sup>18</sup>O firn-core records with summer and winter solstice dates for the core site (linearly interpolating between solstices).<sup>39,40</sup> When the δ<sup>18</sup>O record was ambiguous, the non-sea salt sulfur to sodium ratio summer peak, representing summer solstice, was used to specify the annual maximum δ<sup>18</sup>O. Annual peaks were confirmed using the remaining major ions, for example as shown in Fig. S1.† A modified Abakus® particle counter system was employed in line with the continuous flow analyzer to discern particle concentrations in size bins corresponding to 1.2 to 2.4 μm, 2.4 to 4.5 μm, and 4.5 to 10 μm diameter particles, as described earlier by Simonsen *et al.* 2019.<sup>41,42</sup>

## 2.3 Sectioning for OPE analysis

Cores were stored at −30 °C at our walk-in freezer facility in Burlington, Ontario. The ice core was placed on a stainless steel table lined with methanol-cleaned aluminum foil in a −18 °C room where it was further sectioned by hand using a cleaned hack saw. Core sections were transferred to a 4 L pre-cleaned glass bottle for melting. All handlers wore latex gloves and kept direct contact with the core to a minimum. The measured water equivalents, depth of firn core and assigned years are presented in Tables S6 and S7 in the ESI.†



## 2.4 Target OPE analytes

All OPE analytes, abbreviations, full names, and Chemical Abstract Registry Numbers are presented in Table S1 (ESI).<sup>†</sup> The majority of OPE standards were obtained from Sigma Aldrich: triethyl phosphate (TEP, 99.8%), tris(2-chloro-ethyl) phosphate (TCEP, 97%), triphenylphosphine oxide (TPPO), tripropyl phosphate (TPrP, 99%), tris(2,3-dibromopropyl) phosphate (TDBrPP, 99%), tributyl phosphate (TnBP, 99%), triisobutyl phosphate (TiBP, 99%), tris(2-butoxyethyl) phosphate (TBOEP, 94%), tributylphosphine oxide (TBPO, 95%), dioctylphenyl phosphonate (DOPP, 95%), tris(2-ethylhexyl) phosphate (TEHP, 97%), 2-ethylhexyl diphenyl phosphate (EHDPP, 98%). Tetraethylethylene diphosphonate (TEEDP, 97%) was obtained from Fluka and tris(2-chloroisopropyl) (TCPP, 98%), tris(1,3-dichloroisopropyl) phosphate (TDCPP, 96%) from Reidel. Triphenylphosphate (TPP), trixylyl phosphate (TXP), tris(2-isopropylphenyl) phosphonate (T2IPP), and ortho-, meta-, and para-tolyl phosphate isomers (TOTP) were obtained from Wellington Labs. Bis(*tert*-butylphenyl) phenyl phosphate (DTBPP, 95%), 4-(*tert*-butyl)phenyl diphenyl phosphate (TBDPP, 95%), tris(*p*-*tert*-Butylphenyl) phosphate (TTBPP, 95%) were from Angene Chemical. Iso-decyl diphenyl phosphate (iDeDPP) was obtained from Accustandard. Diphenyl-isopropylphenyl phosphate (DIPIPP) was added to the analysis of Mt. Oxford ice core. Fourteen isotopically labeled substances were used as internal standards and are listed in Table S2.<sup>†</sup>

## 2.5 Analysis of OPEs

Extraction of each 500 ml melted annual layer was by solid phase extraction (SPE) using previously published methods.<sup>15,43</sup> Samples were not filtered prior to SPE due to the priority of avoiding possible contamination through contact with filter media. The SPE cartridges (1 ml 60 mg HLB, Waters) were conditioned using 2 ml isopropanol (B&J Honeywell), and 5 ml HPLC grade water (Fisher Scientific). Samples were spiked with 30  $\mu$ l of the internal standard (final 1 ng ml<sup>-1</sup> concentration in extract) and then loaded at 1 ml min<sup>-1</sup>. After loading the cartridge was washed with 3 ml 5% methanol (HPLC grade, Fisher) in water before drying the cartridge under vacuum for 15 minutes. The cartridge was eluted with 5 ml 90/10 methyl *tert* butyl ether (Omnisolv grade, EMD)/methanol. The final extract was evaporated to just dryness using ultra high purity nitrogen and then reconstituted in 0.5 ml acetonitrile (Optima grade, Fisher) for OPE analysis by ultra high performance liquid chromatography tandem mass spectrometry (UHPLC-MS/MS).

Previous analytical methods for OPE was reported<sup>15</sup> and described briefly here. The UHPLC-MS/MS system consisting of a Waters Acquity LC coupled to a Waters Xevo TQS tandem mass spectrometer with conditions as previously reported.<sup>15</sup> Analytes were separated using a BEH C18 column (1.7  $\mu$ m, 50  $\times$  1 mm) in a 60 °C thermostatted compartment using a water (A) and methanol (B) mobile phase, both containing 0.1% formic acid, gradient and constant flow rate of 0.3 ml min<sup>-1</sup>. Further details on the UHPLC-MS/MS parameters can be found in the ESI (Tables S1 and S2).<sup>†</sup>

Analysis of contaminants in ice cores requires clean handling procedures during sampling, sectioning and extraction. A detailed elaboration of OPE contamination potential during field sampling and laboratory processing as well as the controls that were administered, are presented in the ESI.<sup>†</sup> Field blanks were based on handling, transport and exposure of laboratory water from the Polar Continental Shelf Program (PCSP) research facility Resolute Bay, NU, Canada to the field sites in comparison to the same water kept in the laboratory at PCSP. We applied laboratory method blanks, consisting of the SPE process without sample. Precision was evaluated based on duplicate extraction and analysis of 12 ice sections that had large enough volume to split into two samples. Recovery was evaluated using extraction efficiency (EE) using a composite of ice core melted water. The composite was prepared by combining subsamples of melted ice sections (*i.e.* excess sample from each discrete melted sample bottle). To assess EE, one 500 ml aliquot composite sample was spiked native and internal standards prior to extraction (pre-extraction spiked sample). These data were then compared to an unspiked 500 ml composite sample that was extracted to produce a final extract, which was then spiked with native and internal standards just before instrument analysis (*i.e.* post-extraction spike). Deviation in analyte peak area between the pre-extraction spike and the post-extraction spike would be due to extraction efficiency because both samples have the same matrix (Table S4<sup>†</sup>). Accuracy was evaluated by comparing the calculated concentrations recovered in spiked samples to the theoretical spike. Quantitation was based on calibration curves using relative response of the native standard to corresponding internal standard. For analytes lacking an analogous isotopically labeled standard, the internal standard with the closest retention time was applied (Table S1<sup>†</sup>). The calibration curve consisted of 15 levels: 0.05, 0.1, 0.15, 0.25, 0.3, 0.4, 0.65, 0.95, 1.25, 2.0, 3.0, 4.0, 7.0, 9.0, 12 ng ml<sup>-1</sup> of native standard and 1 ng ml<sup>-1</sup> of internal standard. This research group participated in two international interlaboratory studies for 16 different OPE congeners analysis and yielded excellent accuracy based on zeta-scores corresponding to less than 1.0 as described in our earlier publication<sup>15</sup> and report (lab #3, Supporting Information for Stubbings *et al.*).<sup>44</sup> All aspects pertaining to QA/QC (limits of detection, recovery, interlaboratory results) are presented in the ESI (Tables S4 and S5).<sup>†</sup>

## 2.6 Statistical analysis

All concentrations are reported in units of nanogram per litre (ng L<sup>-1</sup>). Owing to unfiltered samples being extracted, all sample concentrations represent bulk water and particles. Descriptive statistical analyses are presented for OPEs in both sites. Detection frequency (DF) for each analyte was expressed as percentage of samples with >MDL concentration per site. Arithmetic mean and standard error were calculated for analytes with >50% DF. For these analytes, <MDL concentrations were substituted using the maximum likelihood estimation approach.<sup>45</sup> Given that sampling in both sites occurred in the month of May, concentration and flux calculations in the upper layer does not include the full year of accumulation and only 5.5 months.



### 3 Results

#### 3.1 Concentration profile of OPEs in arctic ice

OPEs were detected in every annual layer from 1979 to 2015 in Devon Ice Cap and 1975 to 2017 in Mt. Oxford icefield. Concentration data for both ice cores are summarized in Table 1 and shown in Tables S6 and S7 in the ESI.† The composition profiles of OPEs can be generalized in 10 year intervals in Fig. 2. In the ice sections representing the few years, 2010–2014 in Devon Ice Cap and 2010–2016 in Mt. Oxford icefield, the major OPEs based on concentration were the chlorinated OPEs, 40–42% TCPP ( $58 \pm 10 \text{ ng L}^{-1}$  in Mt. Oxford and  $184 \pm 62 \text{ ng L}^{-1}$  in Devon), 4–5% TCEP ( $7.8 \pm 1.9 \text{ ng L}^{-1}$  in Mt. Oxford and  $18 \pm 3 \text{ ng L}^{-1}$  in Devon), 2–4% TDCPP ( $5.1 \pm 0.8 \text{ ng L}^{-1}$  in Mt. Oxford and  $7.7 \pm 0.9 \text{ ng L}^{-1}$  in Devon), the alkyl OPEs 4–27% TBOEP ( $39 \pm 7 \text{ ng L}^{-1}$  in Mt. Oxford and  $17 \pm 2 \text{ ng L}^{-1}$  in Devon), and 4–18% TEP ( $5.1 \pm 1.0 \text{ ng L}^{-1}$  in Mt. Oxford and  $18 \pm 2 \text{ ng L}^{-1}$  in Devon). The linear tributyl phosphate ester isomer, TnBP, was more prevalent in Devon Ice Cap ( $5.2 \pm 1.6 \text{ ng L}^{-1}$  in Mt. Oxford and  $29 \pm 3 \text{ ng L}^{-1}$  in Devon) than the isopropyl isomer (TiBP), as was TPP ( $3.7 \pm 0.7 \text{ ng L}^{-1}$  in Mt. Oxford and  $155 \pm 79 \text{ ng L}^{-1}$  in Devon) (Fig. S2, ESI†). In the Mt. Oxford icefield, TiBP was more prevalent ( $14 \pm 2 \text{ ng L}^{-1}$  in Mt. Oxford and  $1.2 \pm 0.1 \text{ ng L}^{-1}$  in Devon). The predominance of these OPEs is consistent with international chemical inventory data, such as 2013–2015 inventory in Canada, reporting 1–10 M kg TCPP, 0.1–1 M kg for TEP, TPP, and TDCPP and  $10^4$ – $10^5$  kg for TBOEP in 2013. The US inventory 2020 chemical data reporting (CDR) database is not based on SI units and instead reports quantities in pounds (lbs), however, an approximate conversion to kilograms is provided. The CDR data

corresponded to 20–100  $\times 10^6$  lbs TCPP (approximately  $9.1 \times 10^6$  kg to  $45 \times 10^6$  kg), 1–20  $\times 10^6$  lbs TDCPP (approximately  $0.45 \times 10^6$  kg to  $9.1 \times 10^6$  kg), 1–20  $\times 10^6$  lbs TBOEP, 1–10  $\times 10^6$  lbs TEP, 1–10  $\times 10^6$  lbs TPP and 1–10  $\times 10^6$  lbs TnBP national production volume per year.<sup>46,47</sup> In the same database TiBP is also listed but with a national production volume corresponding to  $<1 \times 10^6$  lbs per year (*i.e.*  $<450\,000$  kg Table S3†). According to European Regulation on Registration, Evaluation, Authorisation and Restriction of Chemicals (REACH) data in 2013, TEP, TEHP, TBOEP, and TDCPP all had production and import inventories in the range of 1000– $10^4$  kg. The predominance of TCPP post-2011 may be due in part that it has been used as a replacement for TCEP since TCEP has been restricted under REACH legislation.<sup>48</sup>

We are cognizant of the possible impact of post-depositional processes on the profile of OPEs detected in ice cores such as melting, percolation, volatilization, and transformation. For example, Prats *et al.* 2022 interpreted the temperature-dependence gas phase concentrations of OPEs in the Pyrenees mountain range to be suggestive of volatilization from snow to air.<sup>49</sup> However, there is uncertainty whether all OPEs are impacted as they observed a statistically-significant inverse temperature dependence on air concentrations for TCEP, TCPP and TPP but not TnBP nor TDCPP.<sup>49</sup> In polar regions, consistently low temperatures should limit the occurrence of volatilization and may also limit their transformation, which is further supported by polar air sampling studies reporting OPEs existing primarily in the particle phase as opposed to gas-phase.<sup>50</sup>

These particular OPEs (TCEP, TCPP, TDCPP, TBOEP, TiBP, TnBP, and TPP) are predominant in other atmospheric samples including precipitation from Frankfurt, Germany<sup>4</sup> and Albany,

**Table 1** Summary of OPEs concentrations, listed with chemical abstract service registry number (CAS RN), in annual ice core sections from Devon Ice Cap and Mt. Oxford icefield: detection frequency (DF, %), median (med,  $\text{ng L}^{-1}$ ), arithmetic mean ( $\text{ng L}^{-1}$ ), standard error (SE,  $\text{ng L}^{-1}$ ), maximum concentration (MAX,  $\text{ng L}^{-1}$ ), method detection limit (MDL,  $\text{ng L}^{-1}$ )

|                                | TEP     | TnBP     | TiBP     | TPPO     | TCEP     | TCPP        | TDCPP       | TEEDP            | TPP      | EHDPP     | TOTP             | iDeDPP      | TBOEP   | TXP              | TEHP             | DTBPP       | T2iPP       | TBDPP            | DIPIPP          |
|--------------------------------|---------|----------|----------|----------|----------|-------------|-------------|------------------|----------|-----------|------------------|-------------|---------|------------------|------------------|-------------|-------------|------------------|-----------------|
| CAS RN                         | 78-40-0 | 126-73-8 | 126-71-6 | 791-28-6 | 115-96-8 | 13 674-84-5 | 13 674-87-8 | 995-32-4         | 115-86-6 | 1241-94-7 | 1330-78-5        | 29 761-21-5 | 78-51-3 | 25 155-23-1      | 78-42-2          | 65 652-41-7 | 64 532-95-2 | 56 803-37-3      | 69 515-46-4     |
| <b>Devon ice cap, n = 36</b>   |         |          |          |          |          |             |             |                  |          |           |                  |             |         |                  |                  |             |             |                  |                 |
| DF <sup>a</sup>                | 100     | 100      | 100      | 100      | 100      | 100         | 100         | 69               | 100      | 100       | 100              | 100         | 100     | 83               | 47               | 83          | 86          | 12               | NA <sup>b</sup> |
| MED                            | 8.2     | 11       | 0.68     | 0.61     | 6.0      | 22          | 3.4         | 0.094            | 12       | 0.38      | 0.10             | 0.26        | 10      | 0.014            | <MDL             | 0.045       | 0.099       | <MDL             |                 |
| MEAN                           | 9.1     | 14       | 0.71     | 0.89     | 8.4      | 73          | 4.1         | 0.17             | 37       | 0.45      | 0.15             | 0.58        | 12      | 0.023            | N/A <sup>c</sup> | 0.082       | 0.52        | N/A <sup>c</sup> |                 |
| SE                             | 0.8     | 1.3      | 0.05     | 0.15     | 0.9      | 20          | 0.4         | 0.03             | 15       | 0.05      | 0.03             | 0.03        | 0.1     | 0.003            | N/A <sup>c</sup> | 0.017       | 0.23        | N/A <sup>c</sup> |                 |
| MAX                            | 28      | 33       | 1.8      | 6.7      | 31       | 633         | 12          | 1.1              | 552      | 1.9       | 1.1              | 2.9         | 46      | 0.11             | 0.11             | 0.74        | 9.8         | 3.6              | NA <sup>b</sup> |
| MDL                            | 0.12    | 0.081    | 0.031    | 0.051    | 0.22     | 0.49        | 0.22        | 0.015            | 0.12     | 0.027     | 0.0062           | 0.36        | 0.58    | 0.001            | 0.056            | 0.0031      | 0.0017      | 0.075            |                 |
| <b>Oxford icefield, n = 43</b> |         |          |          |          |          |             |             |                  |          |           |                  |             |         |                  |                  |             |             |                  |                 |
| DF <sup>a</sup>                | 95      | 100      | 100      | 81       | 98       | 100         | 100         | 19               | 100      | 100       | 44               | 98          | 100     | 2                | 100              | 100         | 51          | 89               | 98              |
| MED                            | 3.3     | 3.0      | 7.4      | 0.14     | 3.1      | 34          | 2.6         | <MDL             | 1.3      | 1.6       | <MDL             | 0.58        | 21      | <MDL             | 0.36             | 0.13        | 0.024       | 0.31             | 0.023           |
| MEAN                           | 3.6     | 3.2      | 8.5      | 0.19     | 3.8      | 38          | 3.5         | N/A <sup>c</sup> | 1.9      | 1.9       | N/A <sup>c</sup> | 0.71        | 22      | N/A <sup>c</sup> | 0.50             | 0.20        | 0.064       | 0.41             | 0.029           |
| SE                             | 0.3     | 0.3      | 0.8      | 0.03     | 0.5      | 5           | 0.4         | N/A <sup>c</sup> | 0.2      | 0.2       | N/A <sup>c</sup> | 0.08        | 2       | N/A <sup>c</sup> | 0.06             | 0.04        | 0.018       | 0.05             | 0.004           |
| MAX                            | 11      | 15       | 26       | 1.01     | 20       | 182         | 17          | 0.13             | 6.8      | 5.3       | 12               | 2.3         | 75      | 0.30             | 2.23             | 1.32        | 0.65        | 1.96             | 0.14            |
| MDL                            | 0.44    | 0.21     | 0.085    | 0.21     | 0.53     | 1.7         | 0.39        |                  | 0.16     | 0.11      | 0.16             | 0.047       | 0.88    | 0.021            | 0.0046           | 0.013       | 0.017       | 0.075            |                 |

<sup>a</sup> Detection frequencies were 31% for TBPO (CAS RN 814-29-9) in Devon and 7.0% in Oxford, 0% for TDBrPP (CAS RN 126-72-7) in both locations, 25% for DOPP in Devon and 0% in Oxford and 17% for TTBPP in Devon and 39% in Oxford. <sup>b</sup> NA – not available; DIPIPP was not a targeted analyte for Devon Ice Cap. <sup>c</sup> N/A – not applicable. Arithmetic mean and standard error were not calculated for analytes with detection frequency  $<50\%$ .



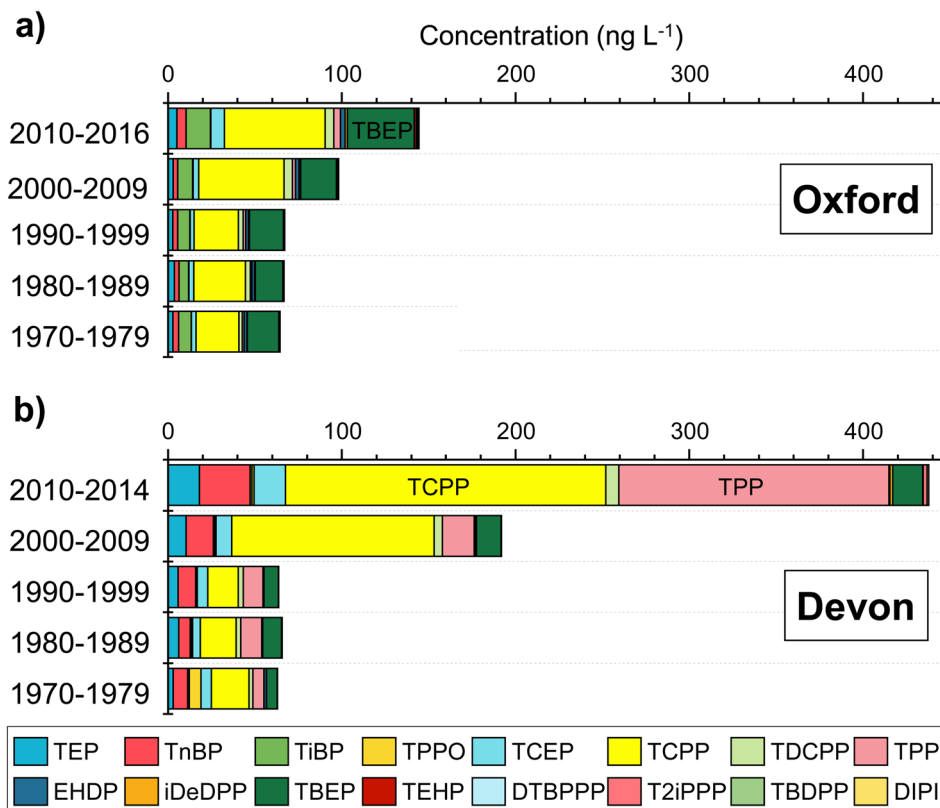


Fig. 2 Multi-year binned average OPEs concentrations,  $\text{ng L}^{-1}$  in ice cores from (a) Mt. Oxford icefield and (b) Devon Ice Cap. Note that sampling year does not represent annual accumulation for Devon Ice Cap in 2015 and Mt. Oxford icefield in 2017.

New York.<sup>51</sup> Though Albany, NY and Frankfurt, Germany are highly populated and urban at latitudes approximately  $33\text{--}45^\circ$  south of Devon Ice Cap, OPE rainwater concentrations are similar to 2015 Devon Ice Cap ice concentrations. For example, median Frankfurt precipitation *versus* 2015 Devon Island ice corresponded to:  $71$  vs.  $31$   $\text{ng L}^{-1}$  TCEP,  $403$  vs.  $158$   $\text{ng L}^{-1}$  TCPP,  $4$   $\text{ng L}^{-1}$  vs.  $12$   $\text{ng L}^{-1}$  TDCPP, and  $21$   $\text{ng L}^{-1}$  vs.  $24$   $\text{ng L}^{-1}$  TBOEP.<sup>4</sup> In precipitation from Albany, mean concentrations were  $5.7$   $\text{ng L}^{-1}$  TCEP,  $62$   $\text{ng L}^{-1}$  TCPP,  $12$   $\text{ng L}^{-1}$  TDCPP, and  $41$   $\text{ng L}^{-1}$  TBOEP and akin to the Devon Ice Cap, TDBPP and EHDPP were  $<\text{MDL}$ . In snow of the Laohugou and Hailuogou glaciers in the Tibetan Plateau, the ranked prominence of OPE congeners corresponded to TCEP, TCPP, TDCPP, TPP, TEP, and TnBP and the chlorinated OPEs accounted for 83% of the OPE profile.<sup>10</sup> The similarity in OPE compositional profile in precipitation from urban centres may support the hypothesis of long range transport. While the similarity in absolute concentrations is also interesting, depositional flux is preferred for spatial comparisons.

The spatial pattern of OPEs in Arctic air has been developed from research over the last decade. Several studies used passive air samples and report air concentrations representing combined gas and particle phase concentrations. In the eastern Arctic, between Svalbard and East Greenland,  $\sum_8\text{OPEs}$  concentration ranged from  $50\text{--}100$   $\text{pg m}^{-3}$ , with 95% of the concentration profile attributed to TCEP and TCPP.<sup>52</sup> In air from Longyearbyen on Svalbard, Salamova *et al.* observed

a predominance of TnBP (median  $56$   $\text{pg m}^{-3}$ ), TCPP ( $57$   $\text{pg m}^{-3}$ ), and  $63$   $\text{pg m}^{-3}$  TBOEP, though it should be noted that the sampling site was on top of the University Centre and cannot be considered a remote site.<sup>12</sup> Similarly, in Ny-Ålesund on Svalbard, Li *et al.* (2022) reported mean air concentrations of  $110$   $\text{pg m}^{-3}$  TCEP,  $55$   $\text{pg m}^{-3}$  TCPP and  $71$   $\text{pg m}^{-3}$  TnBP.<sup>53</sup> Sühring *et al.* detected OPEs in air from the Canadian Arctic that demonstrated higher concentrations of OPEs in air associated with local point sources. For example, near the community of Resolute Bay (population 198) on Cornwallis Island, land-based air samples in 2012 had  $>2000$   $\text{pg m}^{-3}$  TnBP at  $74.70^\circ\text{N}$ ,  $94.83^\circ\text{W}$  whereas in the ship-based air sampling near the same location ( $74.42^\circ\text{N}$ ,  $95.07^\circ\text{W}$ ), TnBP was less than detection limits.<sup>13</sup> Möller *et al.* also measured OPEs in the air mass above in the Bering and Chukchi Seas, near Alaska and Russia sampled onboard the research ice-breaker Xuelong (Snow Dragon):  $85\text{--}529$   $\text{pg m}^{-3}$  TCPP and  $126\text{--}585$   $\text{pg m}^{-3}$  TCEP as the major OPEs compared to  $<\text{LOD} - 5$   $\text{pg m}^{-3}$  TDCPP,  $16\text{--}35$   $\text{pg m}^{-3}$  TiBP, and  $<\text{LOQ} - 36$   $\text{pg m}^{-3}$  TnBP.<sup>54</sup> A similar cruise was conducted on the Xuelong in the Bering Strait and Chukchi Sea more recently in 2018 confirmed the prevalence of TCEP and TCPP in air samples.<sup>14</sup> OPEs are also present in Antarctic air as confirmed recently by Hao *et al.* who reported the concentration of 7 OPE congeners in XAD-resin based passive air samplers in the Fildes Peninsula, West Antarctica.<sup>50</sup> The same OPE congeners reported in this study were also detected in our samples: TnBP, TEHP, EDPP, TPP, TCPP, TDCPP, and TCEP.



In addition to OPE measurements in air samples in the Arctic, there have been a few cruises that also analyzed OPEs in water bodies in the Arctic. For example, McDonough *et al.* confirmed ocean circulation of OPEs in the Arctic through deployment of passive samplers in various locations in the Canadian Arctic Ocean and deep water in the Fram Strait with median water concentrations corresponding to 26 ng L<sup>-1</sup> TnBP, 1200 ng L<sup>-1</sup> TCEP, 166 ng L<sup>-1</sup> TCPP, 114 ng L<sup>-1</sup> TDCPP, 5 ng L<sup>-1</sup> TPP and <LOD for TDBPP.<sup>55</sup> The detection of OPEs in marine water and air suggest long range transport potential of OPEs.

Very high concentrations of TCPP were measured in the ice section from 2000 in Devon Ice Cap. This sample was extracted and analyzed twice and consistently high concentrations were measured in the duplicates (525–633 ng L<sup>-1</sup>), representing 84% of the total OPEs for the year 2000. This was an atypical year since TCPP was 58 ng L<sup>-1</sup> in 1999 and 67 ng L<sup>-1</sup> in 2001. The cause for such a high TCPP concentration in the section corresponding to the year 2000 in the Devon Ice Cap is unknown. For the same time period in the Mt. Oxford icefield ice core, the TCPP concentration was uniform and did not display a maxima based on a mean ± S.E. concentration of 39 ± 7 ng L<sup>-1</sup> TCPP from 1999 to 2003. This discounted a common air mass source to both locations. One possibility is the contamination could arise from previous researchers including aircraft activity at the summit as there are field camps there each year. We cannot rule out the possibility of high TCPP levels driven by an episodic influx event, albeit curious that only TCPP and TPP were elevated in this sample and not other OPE congeners.

Iso-decyl diphenylphosphate (iDeDPP) was consistently detected in both locations. Reported uses of iDeDPP are as plasticizers and flame retardants in flexible polyvinyl chloride and minor uses in rubber, polyurethane, textile coatings, paint

and pigment. The first environmental measurement of iDeDPP was in 2016 in fish from the Llobregat River in Spain, ranging from not detected to 851 ng g<sup>-1</sup> lipid weight.<sup>56</sup> Detection of iDeDPP in ice cores, further confirm its emission and propensity for atmospheric transport.

### 3.2 Flux of OPEs to the Arctic

Similar to contaminant analysis in sediment cores, ice core concentrations must be transformed to flux to ascertain temporal trends due to the inter-annual variation in accumulation. It is also best practice to compare spatial contaminant deposition based on flux and not concentration. Annual flux ( $F$  in year  $x$ , ng m<sup>-2</sup> y<sup>-1</sup>), was calculated using eqn (1) by multiplying the OPE concentration ( $C_{\text{OPE}}$ , ng L<sup>-1</sup>) by the accumulation, based on total melted volume of sample ( $V$  in Litres) in that year and the radius of the corer ( $r$  in metres):

$$F_{\text{OPE},x} = \frac{C_{\text{OPE}} \times V_x}{\pi r^2} \quad (1)$$

Fluxes of OPEs to Devon Ice Cap and Mt. Oxford icefield are presented in Fig. 3. The fluxes are relatively high compared to other contaminant classes. In our previous research, we reported maximum fluxes of >C4 PFAS homologues corresponding to 10–150 ng m<sup>-2</sup> y<sup>-1</sup> in Devon Ice Cap cores obtained through the same sampling effort. In comparison, we report OPE congener fluxes as high as 100 000 ng m<sup>-2</sup> y<sup>-1</sup>. Na *et al.* estimated daily dry deposition fluxes of 70 ng m<sup>-2</sup> d<sup>-1</sup> for TCPP and 20 ng m<sup>-2</sup> d<sup>-1</sup> for TCEP based on their measurements in western Arctic air particulate *via* ship-based summertime sampling.<sup>14</sup> This is consistent with our observations of annual OPEs flux on the order of μg m<sup>-2</sup>.

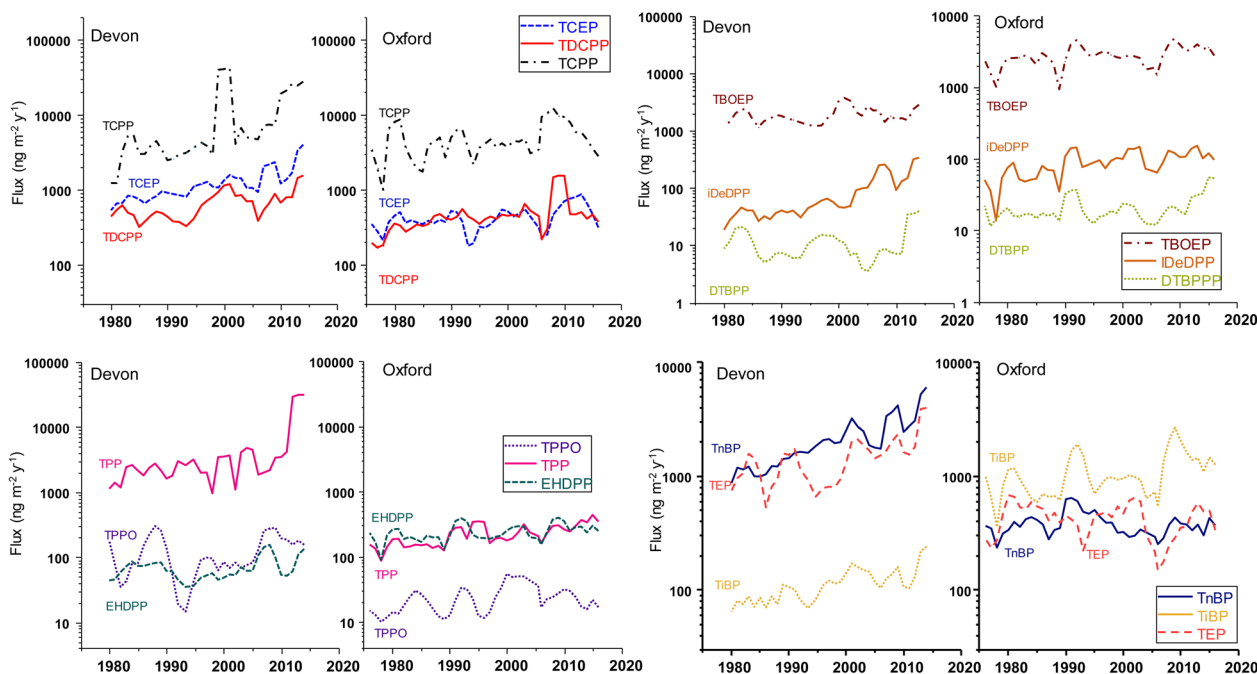


Fig. 3 OPEs fluxes (ng m<sup>-2</sup> y<sup>-1</sup>) in Devon Ice Cap (1979–2014) and Mt. Oxford icefield (1975–2016).



In general, the majority of OPEs in Devon Ice Cap display an exponentially increasing depositional flux from 1979 to 2014. Using the slope from the natural log transformed flux *versus* time, doubling times were estimated for OPEs in Devon Ice Cap (Table S10†). The majority of the OPEs had doubling times between 10 and 35 years. The shortest doubling times corresponded to  $10 \pm 1.3$  y for iDeDPP and  $11 \pm 2.6$  y for TCPP in the Devon Ice Cap.

Interestingly, we do not see the increasing temporal trend in TCPP coincide with a diverging trend in TCEP and TDCPP but rather all three chlorinated OPE congeners increasing ensemble (Table S8†). The magnitude and rate of TCPP accumulation was larger than that of TDCPP and TCEP. This is generally consistent with reports of halogenated OPEs production shifting to TCPP as an alternative to TCEP and TDCPP, given recent legislation on TCEP and TDCPP. The State of California in USA under Proposition 65 has designated TCEP and TDCPP as carcinogens and the European Chemicals Agency has listed TCEP as a substance of high concern.<sup>57</sup> Since 2011, five U.S. states have introduced legislation restricting the use of TDCPP and TCEP in children's products and in 2014, TCEP was prohibited in polyurethane foam in products for children in Canada.<sup>57</sup> Thus, the depositional trends observed here seem to reflect the general usage shift to chlorinated OPEs (TCEP, TDCPP, and TCPP) and non-chlorinated aryl OPEs (*i.e.* TPP and EHDPP) as alternatives to penta-BDE (brominated diphenyl ether).<sup>58</sup>

At the Mt. Oxford site, the temporal trends varied. For TEP, TnBP, and TBOEP, fluxes did not present a statistically significant trend over 3 decades. Other OPEs demonstrated a significant linear (*i.e.*, zero-order) rate of increase in flux. For example, linear regression of annual flux *versus* year had positive slopes corresponding to  $4.9 \pm 0.8$  ng m<sup>-2</sup> y<sup>-1</sup> for TPP,  $1.9 \pm 0.4$  ng m<sup>-2</sup> y<sup>-1</sup> for iDeDPP,  $1.8 \pm 0.2$  ng m<sup>-2</sup> y<sup>-1</sup> for TEHP,  $1.1 \pm 0.2$  ng m<sup>-2</sup> y<sup>-1</sup> for TBDPP, and  $0.59 \pm 0.01$  ng m<sup>-2</sup> y<sup>-1</sup> DIPIPP. The chlorinated OPEs each had a parabolic trend in flux with increasing flux from the early 2000s and peak fluxes occurring in 2008 for TCPP, 2009 for TDCPP, and 2013 for TCEP, followed by a decline (Fig. S3, ESI†). Global production of TCPP, TDCPP, and TCEP has been high since the 1990s, exceeding 50 000 tonnes.<sup>58</sup> Both TCEP and TDCPP are reportedly replacement flame retardants for polybrominated diphenyl ether (PBDE) mixtures.<sup>59</sup> The penta- and octa-BDE mixtures were largely phased out in 2004 and several BDEs are restricted under the Stockholm Convention on Persistent Organic Pollutants.<sup>60</sup> Environmental sampling in remote regions suggests declines of PBDE occurred in the early 2000s, such as ringed seals (*Pusa hispida botnica*) in the Bothnian Bay in northern Baltic Sea<sup>61</sup> demonstrated a decreasing trend of PBDEs post-2000 and post-2003 in migratory Arctic seabirds from Prince Leopold Island in the Canadian archipelago at 74.033°N, 90.083°W.<sup>62</sup> Houde *et al.* found ΣPBDEs in ringed seals from east Baffin Island increased significantly from 1998 to 2008 and then decreased until the last time point in 2013. However, interestingly in the same study, no clear temporal trends in PBDEs were noted in Resolute Bay ringed seals between 2000 and 2013.<sup>63</sup> This underscores the distinction between contaminant monitoring in marine

mammals *versus* abiotic samples for long term trends. For marine mammals, contaminant trends reflect seawater trends, more than atmospheric deposition but also changes in diet, trophic status, and chemicals that are bioaccumulative. The increasing trends in chlorinated OPEs in Devon Ice Cap and Mt. Oxford icefield starting from the early 2000s coincide with the phase out of PBDE. However, there may be other inputs such as airport related activity driving correlations between TnBP and TCEP on the Devon Ice Cap, dissimilar to observations in Mt. Oxford, as discussed below.

To date, this is the longest temporal record of OPEs in the Arctic. Li *et al.* (2022) reported 7 congeners of OPEs in Svalbard air based on year-long deployments of passive samplers from 2011 to 2019.<sup>53</sup> The temporal trends were based on annual concentrations (the volume of air sampled was not measured) and showed an increasing tendency over the eight-year period. Li *et al.* stated that annual mean concentrations of TCEP and TnBP increased with doubling times of 2.7 and 3.8 years, respectively.<sup>53</sup>

Differences in the OPE composition can likely be attributed to differences in air mass source delivery to the two sites. Tendencies back trajectory analyses in two separate years for the Devon Ice Cap core showed contributions from both European and North American air masses similar to previous studies,<sup>23</sup> whereas the Mt. Oxford icefield core site was less influenced by North American sources (Fig. 4, S4 and S5, ESI†). This is consistent with other studies using long term back trajectory confirming western Russia and central Siberia as major source regions for aerosols to northern Ellesmere Island and Greenland.<sup>64</sup> The use of back trajectory density analyses has its limitations as outlined by Kahl *et al.*<sup>35</sup> In particular, the conditions at the source region must be favourable for emission and mixing to an appreciable height and the chemical must remain in the air column en route to the receptor site. As such, chemical tracers and pollen analysis in ice cores are also informative of source regions. Using chemical tracers, Gogo-Azuma and Koerner also determined Eurasia as the dominant source region for anthropogenic aerosols to Agassiz Ice Cap on Ellesmere Island whereas North America and Eurasia were both sources to the Penny Ice Cap on Baffin Island.<sup>65</sup>

Local sources to both Devon Ice Cap and Mt. Oxford icefield cannot be excluded. In particular, the Devon Ice Cap is 120 km and 300 km away from the settlements of Grise Fjord and Resolute, respectively. The ice coring sites at Devon Ice Cap and Mt. Oxford icefield are 400 km and 500 km from Qaanaaq (77.467°N, 69.231°W), and the Thule air base (76.517°N, 68.716°W) in northwestern Greenland. Qaanaaq is a settlement of approximately 600 people. Previous research has suggested elevated OPEs can be linked to airports (Li *et al.* 2019).<sup>66</sup> TnBP is used in a commercial airline fire-resistant hydraulic fluid<sup>13</sup> and Li *et al.* (2022) noted higher OPE concentrations in air near a local airport in Ny-Ålesund, Svalbard.<sup>53</sup> In our earlier study, we reported elevated concentrations (49–100 ng L<sup>-1</sup>) of ΣOPEs in lake water near Resolute Bay, particularly TCEP and TnBP, likely due to the local airport (Sun *et al.* 2020).<sup>15</sup> However, the OPEs profile in Lake Hazen in northern Ellesmere Island downstream of Mt. Oxford icefield, was similar to other remote Arctic





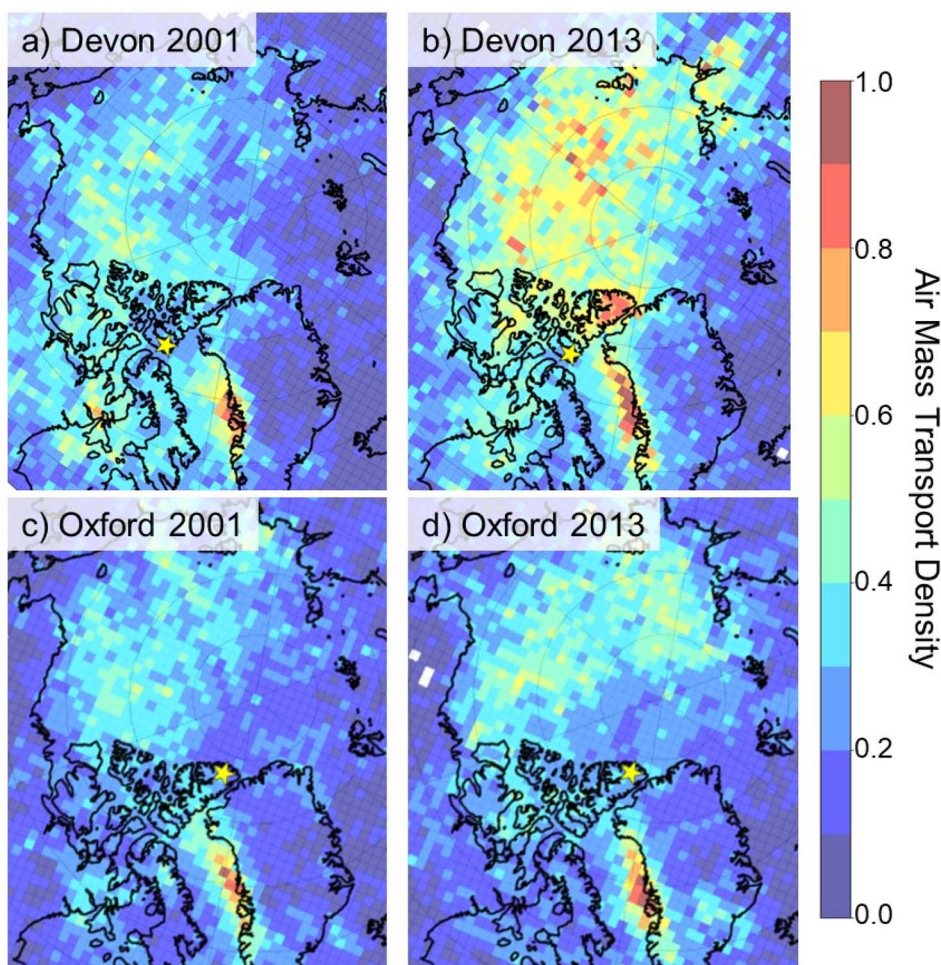


Fig. 4 Air mass transport density (scaled 0 to 1) for air parcels reaching ice coring sites (indicated by star) on the Devon Ice Cap and Mt. Oxford icefield in 2001 and 2013.

lakes with  $\Sigma$ OPEs corresponding to 5 to 10 ng L<sup>-1</sup>. Air filters from land-based sampling in Resolute Bay also had high concentrations of TnBP (median 416 pg m<sup>-3</sup>) and TCEP (median 135 pg m<sup>-3</sup>) compared to ship-based sampling (<LOD TnBP and 50 pg m<sup>-3</sup> TCEP) in Barrow Strait within 100 km of Resolute.<sup>13</sup>

### 3.3 Correlations between OPE congeners

Many of the OPEs were correlated with each other in both coring sites ( $p < 0.05$ ) (Tables S8 and S9<sup>†</sup>). The strongest correlation was TCEP with TnBP (Spearman correlation coefficient  $R_s = 0.91$ , Fig. S6, ESI<sup>†</sup>), which was only observed in the Devon Ice Cap record and not in Mt. Oxford. TCEP is used as a flame retardant, plasticizer, and viscosity regulator in various types of polymers including polyurethanes, polyester resins, and polyacrylates. TnBP is also used as a plasticizer but not as a flame retardant. Li *et al.* found TCEP was highly correlated with TnBP in Arctic air in Svalbard ( $r > 0.8$ ,  $p < 0.001$ ) and characterized it as unexpected given the opposing uses as well as expected differences in transported pathways.<sup>53</sup> In the Devon Ice Cap, TnBP was significantly correlated with other OPEs: TPP, TiBP, TDCPP

and iDeDPP. In the Mt. Oxford icefield, TnBP occurred at a concentration lower by an order of magnitude compared to Devon Island and it was not correlated with any other OPEs. In Mt. Oxford icefield, one of the strongest correlations was between TiBP and TBOEP ( $R_s = 0.86$ ). The same correlation was detected in Devon Ice Cap but with a lower correlation coefficient ( $R_s = 0.40$ ). Möller *et al.* also found significant positive correlations amongst OPEs in air samples from the northern Pacific Ocean and the Arctic Ocean including a significant correlations of TnBP with TCEP (Pearson correlation coefficient  $R_p = 0.798$ ,  $p < 0.006$ ) and TCPP ( $R_p = 0.91$ ,  $p < 0.00031$ ).<sup>54</sup> They hypothesized that nonhalogenated OPEs like TnBP may have similar atmospheric transport mechanisms to halogenated OPEs such as TCEP and TCPP. In addition, there may be a commonality in source and usage. Interestingly TCEP and TCPP were not correlated in Mt. Oxford icefield but were in the Devon Ice Cap. As mentioned earlier, TCPP is a possible replacement for TCEP and TDCPP in 2011–14. Perhaps continued monitoring of depositional trends in halogenated OPEs within the upper layers of firn will reflect some of the diverging trends in usage in time to come.



### 3.4 Sources of OPEs to the Arctic

Contaminants are deposited to Devon Ice Cap *via* long range atmospheric transport from North America and Eurasia depending on the season.<sup>67,68</sup> Arctic haze episodes occur between December and April in which Arctic atmospheric pollution from mid-latitudes is highest.<sup>69,70</sup> During Arctic winters, particle pollution is highest due to local meteorological factors (minimal wet deposition, stratification and dryness of troposphere).<sup>71</sup> Back trajectories show that air flow during winter is from Eurasia and not North America but for the remainder of the year, particulate pollution is at much lower concentrations.<sup>69</sup> Mt Oxford icefield is likely less influenced by Arctic haze. Earlier research indicates that northern Ellesmere Island receives fewer Arctic haze events compared to research stations in Utqiagvik (previously known as Barrow) in Alaska, Station Nord in Greenland, Tiksi in Russia, and Zeppelin in Svalbard due to katabatic winds from the high mountain range.<sup>72,73</sup> While seasonal deposition is likely to differ and would be useful to elucidate sources, we cannot assess this because we sectioned our ice cores by annum.

Zhang *et al.* suggested that chlorinated OPEs are not expected to undergo long range transport through air (characteristic travel distance (CTD) < 200 km) or water (CTD < 600 km) based on a box model evaluation.<sup>16</sup> These estimates are based on temperature-driven thermodynamic partitioning being the major contributor to long range transport. Kinetic advective phase-transfer processes are also likely to play an important role in global distribution of contaminants for which gas-particle interactions are important.<sup>74</sup>

For example, Friedman and Selin (2016) developed a spatial model describing the distribution of polychlorinated biphenyls in Arctic air using GEOS-Chem modeling, which included temperature-dependent partitioning between gas and particle phases.<sup>75</sup> The observation of OPEs in remote regions, contrary to the predicted CTD, suggests that kinetic advective processes such as continuous removal of OPEs in northward moving air masses *via* wet and dry deposition may indeed be a significant delivery mechanism of OPEs to Arctic ecosystems. This effect has been observed for larger molecular weight polychlorinated biphenyls through sorption to atmospheric particles.<sup>74,75</sup> Several studies have confirmed transport of OPEs *via* air particles in remote regions based on sampling in the Canadian Arctic and European Arctic.<sup>12,13,54</sup> Na *et al.* measured OPE in both gas-phase and particle-bound fraction of air samples in the Bering Strait and Chukchi Sea with the fraction of particle-bound OPE comprising 71–93% of the air sample.<sup>14</sup> Further they noted an increasing contribution of the particle bound OPE fraction along the latitudinal transect as temperatures dropped from the northwest Pacific to the Arctic. Of note, experimental derivation of gas-particle partitioning of OPEs is hindered by the artefacts introduced by glass fibre filters.<sup>13</sup> Thus, while it is very likely that aerosol-mediated transport is relevant to OPEs, the distribution is not fully understood. In general, these observations suggest the northern polar regions may be a sink for OPE *via* long range transport followed by cold condensation.

Sühring *et al.* hypothesized that detection of chlorinated OPEs in Arctic air and seawater reflected their continued use in Asia and North America and also their environmental persistence.<sup>13</sup> Sühring *et al.* also noted that the OECD models for long range transport and persistence were not suited for OPEs as they did not account for episodic atmospheric transport and underestimated environmental half-lives.<sup>76</sup> Recent research has shown that the persistence of OPE when absorbed to air particulate is much longer than when in the gas phase<sup>77,78</sup> introducing some uncertainty regarding the true atmospheric half-lives of OPEs, a quantity used in multi-media partitioning models for atmospheric long range transport estimation.

Thus, we propose that atmospheric aerosols are significant drivers of OPE long range transport to the High Arctic. Castro-Jimenez *et al.* observed OPEs in the atmosphere over the Mediterranean and Black Sea using ship-based aerosol sampling. In that study TCPP was the most abundant OPE, 540 to 2722 pg m<sup>-3</sup> as well as TCEP, TDCPP, TiBP, and TnBP.<sup>79</sup> Meyer *et al.* observed PBDE and hexabromocyclododecane (HBCDD) and BDE-209 in the Devon Ice Cap which are relatively non-volatile and hydrophobic.<sup>22</sup> These contaminants were hypothesized to have deposited from atmospheric transport of particles. Recognizing that sodium is a major tracer for open ocean sea salt and sea ice salt,<sup>80</sup> we find that sodium was not significantly correlated with individual OPE in ice from either site suggesting that marine sources are not major contributors to OPE in Devon Ice Cap. OPEs were also not correlated to tracers of crustal dust such as non-sea salt calcium (<sub>nss</sub>Ca) and magnesium as evidenced by *p*-values > 0.05. In the Devon Ice Cap samples, *p*-values and Spearman correlation coefficients for OPEs with <sub>nss</sub>Ca were 0.18 < *p* < 0.98 (−0.0035 < *R*<sub>s</sub> < 0.30) and with Mg were 0.22 < *p* < 0.94 (−0.20 < *R*<sub>s</sub> < 0.27). In Mt. Oxford samples, *p*-values and Spearman correlation coefficients for OPEs with <sub>nss</sub>Ca were 0.13 < *p* < 0.94 (−0.15 < *R*<sub>s</sub> < 0.25) and with Mg were 0.23 < *p* < 0.98 (−0.048 < *R*<sub>s</sub> < 0.19).

Several OPEs were significantly correlated to particle concentrations in the two highest size fractions, comprising 2.4 to 10 μm diameters (Fig. S7 and Table S11 ESI<sup>†</sup>) in both coring sites. In the Devon Ice Cap, the OPEs that were significantly correlated to the particle concentrations were TnBP, TiBP, TCEP, EHDPP, and iDeDPP with *R*<sub>s</sub> corresponding to 0.31 to 0.54 and *p* < 0.05. In the Mt. Oxford icefield, many of the same OPEs were correlated with particles: TnBP, TCEP, EHDPP, iDeDP, but not TiBP. Other OPEs were also correlated with particles in Mt. Oxford icefield: TEP, TPP, TBOEP, TEHP, DTBPP, T2iPP, and TBDPP. Insoluble particles in the ice core were determined using a laser sensor that determines light blockage attributed to insoluble particles in calibrated size bins. The exact composition of the insoluble particle cannot be discerned using this type of analysis and much of the literature<sup>38,81,82</sup> attribute their identity to dust particles in the glacier, mainly due to horizons with high particle counts coinciding with additional analyses such as Al and Fe (and other crustal tracers) on filters or proxy evidence such as volcanic eruptions. More recent approaches have been developed to determine the geochemistry of insoluble particles in ice cores wherein time of flight mass spectrometry was used to investigate the elemental



composition of dust particles.<sup>83</sup> However, to the best of our knowledge, methods have not been applied to identify particle materials of anthropogenic origin such as synthetic fibers and microplastics. Given the widespread use of OPE in plastic materials, it is plausible that plastic particles are a vector of OPE to remote regions. Though little is known about the long range atmospheric transport potential of such materials, microplastics have been identified in Arctic snow and ice. In the remote French Pyrenees, Allen *et al.* observed microplastics in alpine atmospheric samples consisting of fragments, fibres and films comprised of polystyrene, polyethylene, polypropylene, polyvinyl chloride and polyethylene terephthalate, largely with diameters less than 25  $\mu\text{m}$ .<sup>84</sup> Microplastics have also been measured in multi-year sea ice throughout the circumpolar Arctic Ocean.<sup>85</sup> Bergman *et al.* reported small (<100  $\mu\text{m}$ ) microplastics in Arctic snow on ice floes in the Fram Strait and Svalbard as well as snow from the Swiss Alps and non-remote area in Bavaria.<sup>86</sup> In that research, marine transport *via* Arctic ice floes to be a vector of microplastics but they also highlight the possibility of airborne transport akin to mineral particles and pollen.<sup>86</sup> Thus taken together, these research findings emphasize the need to characterize anthropogenic particles in Arctic ice and their potential association with contaminants such as OPE.

## 4 Conclusions

In summary we report depositional flux of OPEs to two areas in the Canadian Arctic indicating their ability to undergo long range transport as well as their ubiquitous presence. The more northern and remote site on Ellesmere Island had lower fluxes of OPEs than the Devon Ice Cap. These results suggest the atmospheric lifetime of OPEs is longer than predicted and also that transport to the Arctic may be occurring *via* aerosols including anthropogenic particles. Icefields in the circumpolar Arctic are shrinking due to climate warming and will likely be a source of OPEs through meltwater to downstream locations.

## Author contributions

ADS: conceptualization, methodology, validation, data curation, visualization, supervision and writing the original draft. CJY: conceptualization, methodology, project administration and funding acquisition. CS: formal analysis, methodology, and validation. AC: investigation, formal analysis, methodology, and resources. IL: investigation, methodology, funding acquisition and resources. DCGM and MS: funding acquisition, investigation and resources. All authors contributed writing, review and editing.

## Conflicts of interest

There are no conflicts to declare.

## Acknowledgements

This work was funded by the Northern Contaminants Program (CJY, ADS, MJS, DCGM, IL, ASC), Polar Continental Shelf

Program (CJY, ASC, DCGM, IL), Natural Science and Engineering Research Council Discovery Grant (CJY and MJS) and Northern Research Supplement (MJS, IL). The authors thank Colleen Mortimer and Anja Rutishauser for assistance in sampling on Devon Ice Cap and Jocelyn Hirose on Mt. Oxford icefield. The authors acknowledge Cyril Cook, Heidi Pickard, John MacInnis, and Daniel Persaud for ice core sectioning.

## References

- 1 G.-L. Wei, D.-Q. Li, M.-N. Zhu, Y.-S. Liao, Z.-Y. Xie, T.-L. Guo, J.-J. Li, S.-Y. Zhang and Z.-Q. Liang, Organophosphorus flame retardants and plasticizers: Sources, occurrence, toxicity and human exposure, *Environ. Pollut.*, 2015, **196**, 29–46.
- 2 A. Marklund, B. Andersson and P. Haglund, Screening of organophosphorus compounds and their distribution in various indoor environments, *Chemosphere*, 2003, **53**, 1137–1146.
- 3 A. Bacaloni, F. Cucci, C. Guarino, M. Nazzari, R. Samperi and A. Lagana, Occurrence of organophosphorus flame retardant and plasticizers in three volcanic lakes of central Italy, *Environ. Sci. Technol.*, 2008, **42**, 1898–1903.
- 4 J. Regnery and W. Puttmann, Seasonal fluctuations of organophosphate concentrations in precipitation and storm water runoff, *Chemosphere*, 2010, **78**, 958–964.
- 5 M. B. Woudneh, J. P. Benskin, G. Wang, R. Grace, M. C. Hamilton and J. R. Cosgrove, Quantitative determination of 13 organophosphorous flame retardants and plasticizers in a wastewater treatment system by high performance liquid chromatography tandem mass spectrometry, *J. Chromatogr. A*, 2015, **1400**, 149–155.
- 6 A. K. Greaves, R. J. Letcher, D. Chen, D. J. McGoldrick and S. M. Backus, Retrospective analysis of organophosphate flame retardants in herring gull eggs and relation to the aquatic food web in the Laurentian Great Lakes of North America, *Environ. Res.*, 2016, **150**, 255–263.
- 7 J. D. Meeker, E. M. Cooper, H. M. Stapleton and R. Hauser, Urinary metabolites of organophosphate flame retardants: Temporal variability and correlations with house dust concentrations, *Environ. Health Perspect.*, 2013, **121**, 580–585.
- 8 A. M. Sundkvist, U. Olofsson and P. Haglund, Organophosphorus flame retardants and plasticizers in marine and fresh water biota and in human milk, *J. Environ. Monit.*, 2010, **12**, 943–951.
- 9 W. Cheng, L. Sun, W. Huang, T. Ruan, Z. Xie, P. Zhang, R. Ding and M. Li, Detection and distribution of Tris(2-chloroethyl) phosphate on the East Antarctic ice sheet, *Chemosphere*, 2013, **92**, 1017–1021.
- 10 X. Zou, S. Hou, S. Wu, K. Liu, R. Huang, W. Zhang, J. Yu, Z. Zhan and H. Pang, The first detection of organophosphate esters (OPEs) of a high altitude fresh snowfall in the northeastern Tibetan Plateau, *Sci. Total Environ.*, 2022, **838**, 155615.
- 11 Z. Xie, Z. Wang, O. Magand, A. Thollot, R. Ebinghaus, W. Mi and A. Dommergue, Occurrence of legacy and emerging



- organic contaminants in snow at dome C in the Antarctic, *Sci. Total Environ.*, 2020, **741**, 140200.
- 12 A. Salamova, M. H. Hermanson and R. A. Hites, Organophosphate and halogenated flame retardants in atmospheric particles from a European Arctic site, *Environ. Sci. Technol.*, 2014, **48**, 6133–6140.
- 13 R. Sührling, M. L. Diamond, M. Scheringer, F. Wong, M. Pucko, G. Stern, A. Burt, H. Hung, P. Fellon, H. Li and L. M. Jantunen, Organophosphate Esters in Canadian Arctic Air: Occurrence, Levels and Trends, *Environ. Sci. Technol.*, 2016, **50**, 7409–7415.
- 14 G. Na, C. Hou, R. Li, Y. G. Shi, H. S. Jin, Y. Gao, L. Jiao and Y. Cai, Occurrence, distribution, air-seawater exchange and atmospheric deposition of organophosphate esters (OPEs) from the Northwestern Pacific to the Arctic Ocean, *Mar. Pollut. Bull.*, 2020, **157**, 111243.
- 15 Y. Sun, A. O. De Silva, K. A. St Pierre, D. C. G. Muir, C. Spencer, I. Lehnher, M. J. Sharp, A. O. De Silva and C. J. Young, Ice Core Record of Persistent Short-Chain Fluorinated Alkyl Acids: Evidence of the Impact From Global Environmental Regulations, *Geophys. Res. Lett.*, 2020, **47**, e2020GL087535.
- 16 X. Zhang, R. Sührling, D. Serodio, M. Bonnell, N. Sundin and M. L. Diamond, Novel flame retardants: Estimating the physical-chemical properties and environmental fate of 94 halogenated and organophosphate PBDE replacements, *Chemosphere*, 2016, **144**, 2401–2407.
- 17 I. Liagkouridis, A. P. Cousins and I. T. Cousins, Physical-chemical properties and evaluative fate modelling of 'emerging' and 'novel' brominated and organophosphorus flame retardants in the indoor and outdoor environment, *Sci. Total Environ.*, 2015, **524–525**, 416–426.
- 18 L. Ye, J. Li, S. Gong, S. M. Herczegh, Q. Zhang, R. J. Letcher and G. Su, Established and emerging organophosphate esters (OPEs) and the expansion of an environmental contamination issue: a review and future directions, *J. Hazard. Mater.*, 2023, **459**, 132095.
- 19 A. Lippold, M. Harju, J. Aars, P. Blévin, J. Bytingsvik, G. W. Gabrielsen, K. M. Kovacs, J. L. Lyche, C. Lydersen, A. H. Rikardsen and H. Routti, Occurrence of emerging brominated flame retardants and organophosphate esters in marine wildlife from the Norwegian Arctic, *Environ. Pollut.*, 2022, **315**, 120395.
- 20 C. Yao, H. Yang and Y. Li, A review on organophosphate flame retardants in the environment: Occurrence, accumulation, metabolism and toxicity, *Sci. Total Environ.*, 2021, **795**, 148837.
- 21 J. J. Macinnis, K. French, D. C. G. Muir, C. Spencer, A. Criscitiello, A. O. De Silva and C. J. Young, Emerging investigator series: A 14-year depositional ice record of perfluoroalkyl substances in the High Arctic, *Environ. Sci.: Processes Impacts*, 2017, **19**, 22–30.
- 22 T. Meyer, D. C. G. Muir, C. Teixeira, X. Wang, T. Young and F. Wania, Deposition of brominated flame retardants to the Devon Ice Cap, Nunavut, Canada, *Environ. Sci. Technol.*, 2012, **46**, 826–833.
- 23 H. M. Pickard, A. S. Criscitiello, C. Spencer, M. J. Sharp, D. C. G. Muir, A. O. De Silva and C. J. Young, Continuous non-marine inputs of per- and polyfluoroalkyl substances to the High Arctic: a multi-decadal temporal record, *Atmos. Chem. Phys.*, 2018, **18**, 5045–5058.
- 24 C. J. Young, V. I. Furdul, J. Franklin, R. M. Koerner, D. C. G. Muir and S. A. Mabury, Perfluorinated acids in arctic snow: New evidence for atmospheric formation, *Environ. Sci. Technol.*, 2007, **41**, 3455–3461.
- 25 X. Zhang, T. Meyer, D. C. G. Muir, C. Teixeira, X. Wang and F. Wania, Atmospheric deposition of current use pesticides in the Arctic: Snow core records from the Devon Island Ice Cap, Nunavut, Canada, *Environ. Sci.: Processes Impacts*, 2013, **15**, 2304–2311.
- 26 H. M. Pickard, A. S. Criscitiello, D. Persaud, C. Spencer, D. C. G. Muir, I. Lehnher, M. J. Sharp, A. O. De Silva and C. J. Young, Ice Core Record of Persistent Short-Chain Fluorinated Alkyl Acids: Evidence of the Impact From Global Environmental Regulations, *Geophys. Res. Lett.*, 2020, **47**, e2020GL087535.
- 27 W. Colgan and M. Sharp, Combined oceanic and atmospheric influences on net accumulation on Devon Ice Cap, Nunavut, Canada, *J. Glaciol.*, 2008, **54**, 28–40.
- 28 J. England, I. R. Smith and D. J. A. Evans, The last glaciation of east-central Ellesmere Island, Nunavut: ice dynamics, deglacial chronology, and sea level change, *Can. J. Earth Sci.*, 2000, **37**, 1355–1370.
- 29 E. Steinbring, R. Carlberg, B. Croll, G. Fahlman, P. Hickson, L. Ivanescu, B. Leckie, T. Pfrommer and M. Schoeck, First Assessment of Mountains on Northwestern Ellesmere Island, Nunavut, as Potential Astronomical Observing Sites, *Publ. Astron. Soc. Pac.*, 2010, **122**, 1092–1108.
- 30 A. White and L. Copeland, Area change of glaciers across northern Ellesmere Island, Nunavut, between 1999 and 2015, *J. Glaciol.*, 2018, **64**, 609–623.
- 31 P. P. Dunphy and J. E. Dibb, <sup>137</sup>Cs gamma-ray detection at Summit, Greenland, *J. Glaciol.*, 1994, **40**, 87–92.
- 32 M. Arienzo, J. McConnell, N. Chellman, A. Criscitiello, M. Curran, D. Fritzsche, S. Kipfstuhl, R. Mulvaney, M. Nolan, T. Opel, M. Sigl and J. P. Steffensen, A Method for Continuous <sup>239</sup>Pu Determinations in Arctic and Antarctic Ice Cores, *Environ. Sci. Technol.*, 2016, **50**, 7066–7073.
- 33 A. Criscitiello, T. Geldsetzer, R. Rhodes, M. Arienzo, J. McConnell, N. Chellman, M. Osman, J. Yackel and S. Marshall, Marine aerosol records of Arctic sea-ice and polynya variability from New Ellesmere and Devon Island Firm Cores, Nunavut, Canada, *J. Geophys. Res.: Oceans*, 2021, **126**, 2169–9291.
- 34 A. S. Criscitiello, S. J. Marshall, M. J. Evans, C. Kinnard, A.-L. Norman and M. J. Sharp, Marine aerosol source regions to Prince of Wales Icefield, Ellesmere Island, and influence from the tropical Pacific, 1979–2001, *J. Geophys. Res.: Atmos.*, 2016, **121**, 9492–9507.
- 35 J. D. Kahl, D. A. Martinez, H. Kuhns, C. I. Davidson, J.-L. Jaffrezo and J. M. Harris, Air mass trajectories to Summit, Greenland: A 44-year climatology and some episodic events, *J. Geophys. Res.*, 1997, **102**, 26861–26875.



- 36 B. G. Kopec, X. Feng, E. S. Posmentier and L. J. Sonder, Seasonal deuterium excess variations of precipitation at Summit, Greenland, and their Climatological Significance, *J. Geophys. Res.: Atmos.*, 2018, **124**, 72–91.
- 37 K. Goto-Azuma, R. M. Koerner and D. A. Fisher, An ice-core record over the last two centuries from Penny Ice Cap, Baffin Island, Canada, *Ann. Glaciol.*, 2002, **35**, 29–35.
- 38 J. McConnell, A. Wilson, A. Stohl, M. Arienzo, N. Chellman, S. Eckhardt, E. Thompson, A. Pollard and J. Steffensen, Lead pollution recorded in Greenland ice indicates European emissions tracked plagues, wars, and imperial expansion during antiquity, *Proc. Natl. Acad. Sci. U. S. A.*, 2018, **115**, 5726–5731.
- 39 J. Jouzel, R. B. Alley, K. M. Cuffey, W. Dansgaard, P. Grootes, G. Hoffmann, S. J. Johnsen, R. D. Koster, D. Peel, C. A. Shuman, M. Stievenard, M. Stuiver and J. White, Validity of the temperature reconstruction from water isotopes in ice cores, *J. Geophys. Res.*, 1997, **102**, 26471–26487.
- 40 D. P. Schneider, E. J. Steig and T. Van Ommen, High-resolution ice-core stable isotopic records from Antarctica: towards interannual climate reconstructions, *Ann. Glaciol.*, 2005, **41**, 63–70.
- 41 M. F. Simonsen, G. Baccolo, T. Blunier, A. Borunda, B. Delmonte, R. Frei, S. Goldstein, A. Grinsted, H. A. Kjær, T. Sowers, A. Svensson, B. Vinther, D. Vladimirova, G. Winckler, M. Winstrup and P. Vallelonga, East Greenland ice core dust record reveals timing of Greenland ice sheet advance and retreat, *Nat. Commun.*, 2019, **10**, 4494.
- 42 U. Ruth, D. Wagenbach, J. P. Steffensen and M. Bigler, Continuous record of microparticle concentration and size distribution in the central Greenland NGRIP ice core during the last glacial period, *J. Geophys. Res.: Atmos.*, 2003, **108**, 4098.
- 43 R. Rodil, J. B. Quintana and T. Reemtsma, Liquid chromatography - tandem mass spectrometry determination of nonionic organophosphorus flame retardants and plasticizers in wastewater samples, *Anal. Chem.*, 2005, **77**, 3083–3089.
- 44 W. A. Stubbings, N. Riddell, B. Chittim and M. Venier, Challenges in the analyses of organophosphate esters, *Environ. Sci. Technol. Lett.*, 2017, **4**, 292–297.
- 45 D. Helsel, *Nondetects and Data Analysis: Statistics for Censored Environmental Data*, Wiley, 2005.
- 46 Government of Canada, *Updated Risk Management Scope for 2-Propanol, 1-chloro-, Phosphate (3:1) (TCPP) and 2-Propanol, 1,3-dichloro-, Phosphate 3 (TDCPP)*, 2020.
- 47 Government of Canada, Draft screening assessment flame retardants group, 2021, <https://www.canada.ca/en/environment-climate-change/services/evaluating-existing-substances/draft-screening-assessment-flame-retardants-group.html>.
- 48 E. Verbruggen, J. Rila, T. Traas, C. Posthuma-Doodeman and R. Posthumus, *Environmental Risk Limits for Several Phosphate Esters with Possible Application as Flame Retardant*, RIVM report, 2005, 601501024/2005.
- 49 R. Prats, B. van Droog, P. Fernández and J. Grimalt, Occurrence and temperature dependence of atmospheric gas-phase organophosphate esters in high-mountain areas (Pyrenees), *Chemosphere*, 2022, **292**, 133467.
- 50 Y. Hao, S. Xiong, P. Wang, R. Yang, Z. Pei, Y. Li, Q. Zhang and G. Jiang, Novel brominated and organophosphate flame retardants in the atmosphere of Fildes Peninsula, West Antarctica: Continuous observations from 2011 to 2020, *J. Hazard. Mater.*, 2022, **440**, 129776.
- 51 U.-J. Kim and K. Kannan, Occurrence and Distribution of Organophosphate Flame Retardants/Plasticizers in Surface Waters, Tap Water, and Rainwater: Implications for Human Exposure, *Environ. Sci. Technol.*, 2018, **52**, 5625–5633.
- 52 J. Li, Z. Xie, W. Mi, S. Lai, C. Tian, K.-C. Emeis and R. Ebinghaus, Organophosphate esters in air, snow, and seawater in the North Atlantic and the Arctic, *Environ. Sci. Technol.*, 2017, **51**, 6887–6896.
- 53 Y. Li, S. Xiong, Y. Hao, R. Yang, Q. Zhang, F. Wania and G. Jiang, Organophosphate esters in Arctic air from 2011 to 2019: Concentrations, temporal trends, and potential sources, *J. Hazard. Mater.*, 2022, **434**, 122872.
- 54 A. Möller, R. Sturm, Z. Y. Xie, M. H. Cai, J. F. He and R. Ebinghaus, Organophosphorus flame retardants and plasticizers in airborne particles over the Northern Pacific and Indian Ocean toward the polar regions: evidence for global occurrence, *Environ. Sci. Technol.*, 2012, **46**, 3127–3134.
- 55 C. A. McDonough, A. O. De Silva, C. Sun, A. Cabrerizo, D. Adelman, T. Soltwedel, E. Bauerfeind, D. C. G. Muir and R. Lohmann, Dissolved organophosphate esters and polybrominated diphenyl ethers in remote marine environments: Arctic surface water distributions and net transport through Fram Strait, *Environ. Sci. Technol.*, 2018, **52**, 6208–6216.
- 56 G. Santin, E. Eljarrat and D. Barcelo, Simultaneous determination of 16 organophosphorus flame retardants and plasticizers in fish by liquid chromatography-tandem mass spectrometry, *J. Chromatogr. A*, 2016, **1441**, 34–43.
- 57 E. Schreder, N. Uding and M. La Guardia, Inhalation a significant exposure route for chlorinated organophosphate flame retardants, *Chemosphere*, 2016, **150**, 499–504.
- 58 I. van der Veen and J. de Boer, Phosphorus flame retardants: Properties, production, environmental occurrence, toxicity and analysis, *Chemosphere*, 2012, **88**, 1119–1153.
- 59 H. Stapleton, S. Sharma, G. Getzinger, P. Ferguson, M. Gabriel, T. Webster and A. Blum, Novel and high volume use flame retardants in US couches reflective of the 2005 pentaBDE phase out, *Environ. Sci. Technol.*, 2012, **46**, 13432–13439.
- 60 UNEP, *SC-4/18: Listing of Tetrabromodiphenyl Ether and Pentabromodiphenyl Ether*, United Nations Environmental Program, Stockholm Convention on POPs, 2007.
- 61 F. Bjurlid, A. Roos, I. Ericson Jogsten and J. Hagberg, Temporal trends of PBDD/Fs, PCDD/Fs, PBDEs and PCBs in ringed seals from the Baltic Sea (*Pusa hispida botnica*)



- between 1974 and 2015, *Sci. Total Environ.*, 2018, **616–617**, 1374–1383.
- 62 B. M. Braune, R. J. Letcher, A. J. Gaston and M. L. Mallory, Trends of polybrominated diphenyl ethers and hexabromocyclododecane in eggs of Canadian Arctic seabirds reflect changing use patterns, *Environ. Res.*, 2015, **142**, 651–661.
- 63 M. Houde, X. Wang, S. Ferguson, P. Gagnon, T. Brown, S. Tanabe, T. Kunito, M. Kwan and D. C. G. Muir, Spatial and temporal trends of alternative flame retardants and polybrominated diphenyl ethers in ringed seals (*Phoca hispida*) across the Canadian Arctic, *Environ. Pollut.*, 2017, **223**, 266–276.
- 64 E. Freud, R. Krejci, P. Tunved, R. Leaitch, Q. T. Nguyen, A. Massling, H. Skov and L. Barrie, Pan-Arctic aerosol number size distributions: seasonality and transport patterns, *Atmos. Chem. Phys.*, 2017, **17**, 8101–8128.
- 65 K. Goto-Azuma and R. Koerner, Ice core studies of anthropogenic sulfate and nitrate trends in the Arctic, *J. Geophys. Res.: Atmos.*, 2001, **106**, 4959–4969.
- 66 W. Li, Y. Wang and K. Kannan, Occurrence, distribution, and human exposure to 20 organophosphate esters in air, soil, pine needles, river water, and dust samples collected around an airport in New York State, United States, *Environ. Int.*, 2019, **131**, 105054.
- 67 T. Meyer, D. C. G. Muir, C. Teixeira, X. Wang, T. Young and F. Wania, Deposition of Brominated Flame Retardants to the Devon Ice Cap, Nunavut, Canada, *Environ. Sci. Technol.*, 2012, **46**, 826–833.
- 68 M. Krachler, J. Zheng, R. Koerner, C. Zdanowicz, D. Fisher and W. Shotyk, Increasing atmospheric antimony contamination in the northern hemisphere: snow and ice evidence from Devon Island, Arctic Canada, *J. Environ. Monit.*, 2005, **7**, 1169–1176.
- 69 L. Barrie, Arctic air pollution: An overview of current knowledge, *Atmos. Environ.*, 1986, **20**, 643–663.
- 70 J. Abbatt, W. Leaitch, A. Aliabadi, A. Bertram, J.-P. Blanchet, A. Boivin-Rioux, H. Bozem, J. Burkart, R. Chang, J. Charatte, J. Chaubey, R. Christensen, A. Cirisan, D. Collins, B. Croft, J. Dionne and G. Evans, Overview paper: new insights into aerosol and climate in the Arctic, *Atmos. Chem. Phys.*, 2019, **19**, 2527–2560.
- 71 A. Stohl, Characteristics of atmospheric transport into the Arctic troposphere, *J. Geophys. Res.*, 2006, **111**, D11306.
- 72 P. Quinn, G. Shaw, E. Andrews, E. Dutton, T. Ruoho-Airola and S. Gong, Arctic haze: current trends and knowledge gaps, *Tellus*, 2007, **59B**, 99–114.
- 73 M. Willis, W. Leaitch and J. Abbatt, Processes controlling the composition and abundance of Arctic aerosol, *Rev. Geophys.*, 2018, **56**, 621–671.
- 74 K. J. Hageman, C. Bogdal and M. Scheringer, Chapter 11 Long-Range and Regional Atmospheric Transport of POPs and Implications for Global Cycling, *Compr. Anal. Chem.*, 2015, **67**, 363–387.
- 75 C. Friedman and N. Selin, PCBs in the Arctic atmosphere: determining important driving forces using a global atmospheric transport model, *Atmos. Chem. Phys.*, 2016, **16**, 3433–3448.
- 76 R. Sühling, M. Scheringer, T. F. M. Rodgers, L. M. Jantunen and M. L. Diamond, Evaluation of the OECD POV and LRTP screening tool for estimating the long-range transport of organophosphate esters, *Environ. Sci.: Processes Impacts*, 2020, **22**, 207–216.
- 77 Y. Liu, L. Huang, S. M. Li, T. Harner and J. Liggió, OH-initiated heterogeneous oxidation of tris-2-butoxyethyl phosphate: Implications for its fate in the atmosphere, *Atmos. Chem. Phys.*, 2014, **14**, 12195–12207.
- 78 J. Liu, J. Liggió, T. Harner, L. Jantunen, M. Shoeib and S.-M. Li, Heterogeneous OH Initiated oxidation: a possible explanation for the persistence of organophosphate flame retardants in air, *Environ. Sci. Technol.*, 2014, **48**, 1041–1048.
- 79 J. Castro-Jiménez, N. Berrojalbiz, M. Pizarro and J. Dachs, Organophosphate ester (OPE) flame retardants and plasticizers in the open mediterranean and black seas atmosphere, *Environ. Sci. Technol.*, 2014, **48**, 3203–3209.
- 80 R. Rhodes, X. Yang, E. Wolff, J. McConnell and M. Frey, Sea ice as a source of sea salt aerosol to Greenland ice cores: a model-based study, *Atmos. Chem. Phys.*, 2017, **17**, 9417–9433.
- 81 P. Bohleber, N. Stoll, M. Rittner, M. Roman, I. Weikusat and C. Barbante, Geochemical characterization of insoluble particle clusters in ice cores using two-dimensional impurity imaging, *Geochem., Geophys., Geosyst.*, 2022, **24**, e2022GC010595.
- 82 M. Ram and R. I. Gayley, Insoluble particles in polar ice: Identification and measurement of the insoluble background aerosol, *Geophys. Res. Lett.*, 1994, **21**, 437–440.
- 83 T. Erhardt, C. M. Jensen, O. Borovinskaya and H. Fischer, Single Particle Characterization and Total Elemental Concentration Measurements in Polar Ice Using Continuous Flow Analysis-Inductively Coupled Plasma Time-of-Flight Mass Spectrometry, *Environ. Sci. Technol.*, 2019, **53**, 13275–13283.
- 84 S. Allen, D. Allen, V. R. Phoenix, G. Le Roux, P. Durántez Jiménez, A. Simonneau, S. Binet and D. Galop, Atmospheric transport and deposition of microplastics in a remote mountain catchment, *Nat. Geosci.*, 2019, **12**, 339–344.
- 85 I. Peeken, S. Primpke, B. Beyer, J. Gütermann, C. Katlein, T. Krumpfen, M. Bergmann, L. Hehemann and G. Gerdt, Arctic sea ice is an important temporal sink and means of transport for microplastic, *Nat. Commun.*, 2018, **9**, 1505.
- 86 M. Bergman, S. Mützel, S. Primpke, M. B. Tekman, J. Trachsel and G. Gerdt, White and wonderful? Microplastics prevail in snow from the Alps to the Arctic, *Sci. Adv.*, 2019, **5**, eaax1157.

